SECED 2023 Conference
Earthquake Engineering & Dynamics for a Sustainable Future
14-15 September 2023, Cambridge, UK

NUMERICAL EVALUATION OF KINEMATIC AND INERTIAL LOADS ON PILE-SUPPORTED WHARF STRUCTURES FOUNDED ON LIQUEFIABLE GROUND

Ricardo RODRIGUEZ-PLATA[1], Carlo G. LAI[2]

Abstract: *Damage to seaports during past seismic events has been mainly attributed to the excessive displacement of submerged embankments that have particularly affected pile-supported marginal wharves. Modern building code provisions and guidelines for the seismic design of piles explicitly require de consideration of kinematic and inertial interaction effects. This is customary achieved by the means of simplified static analyses that consider the simultaneous application of the kinematic and inertial loads affected by prescribed weighting factors. The suitability of such factors to account for the different effects expected the pile-deck connections and at the in-ground cross sections of the piles is highly questionable. The present study deals with the estimation of the earthquake design loads for large diameter piles supporting a wharf structure of the port of Gioia Tauro in southern Italy. Fully coupled 2D nonlinear dynamic analysis were conducted in FLAC by considering the non-linear behaviour of the both the liquefiable ground and the superstructure. Kinematic effects were retrieved from the response of the submerged embankment in the absence of the wharf. Results show that the peak bending moment of the piles varies in time and location. For long return periods, the in-phase occurrence of kinematic and inertial effects is shown to be more likely at the pile-deck connections, being the kinematic load predominant and aggravated by inertial effects during the early stages of shaking. Pile-pining effects were also captured, indicating a potential relation between kinematic loads and the displacement field obtained from free-field analysis that could be used for design purposes.*

Introduction

The seismic response of large-diameter pile-supported wharves is a topic of critical importance in geotechnical engineering, particularly in regions with high seismic activity. While previous case studies have mainly focused on small diameter pile-supported wharves in the Pacific basin, little is known about the behavior of larger-diameter pile-supported wharves, commonly found in the Mediterranean. In this context, the present study investigates the seismic response of the deep water wharf at the port of Gioia Tauro in Southern Italy, using time history analyses with the "direct approach" that accounts for both the superstructure and the piles in the same analysis. Advanced constitutive models for liquefiable layers and the superstructure were used in the FLAC 2D commercial code to capture higher-order effects. The response of the liquefiable ground was modelled using PM4SAND, which was calibrated following a CPT-based procedure. The nonlinear response of the wharf was also accounted for by placing plastic hinge zones along the entire length of the piles. In addition, the study examines the kinematic effects by comparing the response of the submerged slope in the presence and absence of the wharf.

This study aims to improve the understanding of the seismic behavior of large-diameter pile-supported wharves and contribute to the development of more accurate and efficient design methodologies. The first two sections refer to the case study and site characterization. The third explains the modelling methodology implemented and the final two sections present the results and discusion in terms of the global and local response of the wharf.

Case study.

The Port of Gioa Tauro is a major transhipment terminal located along the Tyrrhenian coast of the of Reggio Calabria region in southern Italy. Between the years 2000 and 2015 the port mobilized around 3 million TEU per year (Twenty Foot Equivalent Units) placing it among the top 5 transhipment hubs in the Mediterranean basin. It consists of an artificial channel, 220 m wide

[1] IUSS University School for Advanced Studies of Pavia, Pavia, Italy, ricardo.rodriguezplata@iusspavia.it.
[2] Department of Civil Engineering and Architecture, University of Pavia, Pavia, Italy, 3. EUCENTRE, Pavia, Italy.

and 3.8 km long, that extends north-south parallel to the Tyrrhenian cost of the Regio Calabria region (see Figure 1). Most of the berthing operations take place along the eastern bank of the channel, which accommodates three sets of berthing structures, they are highlighted by different shades in Figure 1. Dock BAF, which is the acronym in Italian for “Banchina Alti Fondali” (deep water dock), is a large-diameter pile-supported wharf, built in 2005.

The cross section of wharf BAF is shown in Figure 1, its main components and characteristics are described as follows. The deck is supported by four rows of reinforced concrete piles of 1.5 m of diameter. The leading pile reaches a depth of 40 m from the sea level, while the tips of the trailing and central piles reach depths of 25 m and 30 m respectively. The reinforced concrete deck is 2.4 m tall, and it is composed by 15 segments of 28.8 m length each. The four rows of piles supporting the deck are spaced every 6 m. Tie backs were also installed to provide additional support to the wharf, the information about them is however scarce. Lastly, on the slope of the submerged embankment a 2.6 m thick rip rap layer was installed for scour protection.

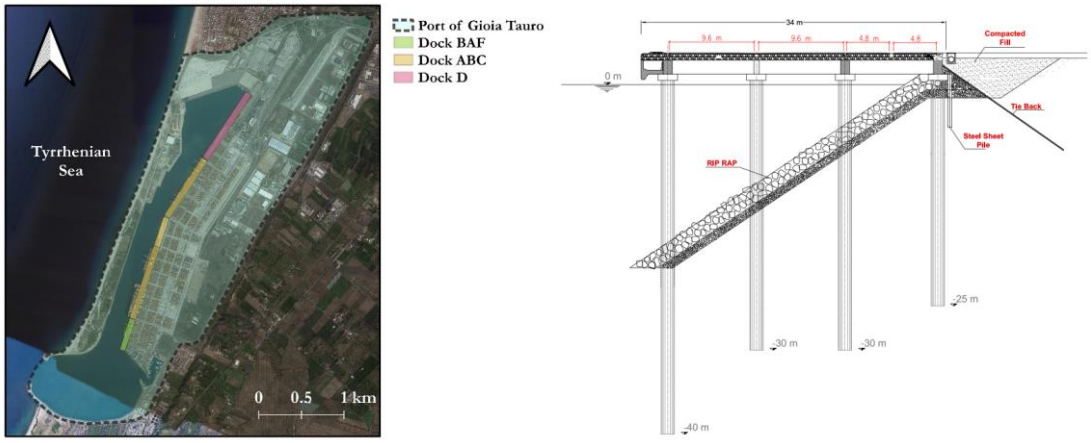

Figure 1. Left panel, Satellite view of the port of Gioia Tauro. Right panel, cross section of the pile-supported wharf of dock BAF.

Subsoil conditions and site characterization.

The port of Gioia is placed on top of a sedimentary deposit of Quaternary age mainly comprised by heterogenous coarse-grained materials which can be found down to 55 to 80m depth (Famà et al., 2014). These granular deposits are underlaid by a thick layer of compacted clay and silty clay which extends down to approximately 600m below the ground surface. As a matter of fact, the mean shear wave velocity of the latter layer was found to be around 800m/s, which was interpreted as the seismic bedrock of the site.

The relevant geotechnical information of the area was obtained from past technical reports and research projects that dealt with the assessment of the liquefaction hazard and seismic risk for the port (Bozzoni et al., 2014; Conca et al., 2020; Faccioli and Vanini, 2003). The information contained in these studies was gathered from SPT, CPT and DMT soundings, as well as from geophysical measurements of compressional and shear wave velocities, and laboratory testing of disturbed samples.

Figure 2 shows the CPT profiles gathered from the tests executed prior to the construction of the wharf by Facciorusso and Vannucchi (2003). The profiles are plotted in terms of normalized clean-sand equivalent tip resistance (q_{c1Ncs}) and soil behaviour type index (I_c) (Boulanger and Idriss, 2014; Robertson and Cabal, K. L., 2015). For the former, reference lines are plotted for q_{c1Ncs} equal to 110, 135 and 155, with respective cyclic resistance ratios (CRR) of 0.15, 0.21 and 0.35. The data indicate that first 20 m of the soil deposit are comprised by coarse-grained materials with varying degree of density. The profile of q_{c1Ncs} indicate the presence of three distinct layers with boundaries at 5- and 12-meters depth approximately. The middle layer, being the densest, is not liquefiable ($q_{c1Ncs} > 200$), while the bottom and upper layers are softer and may exhibit cyclic mobility behaviour or liquefaction.

The upper most layer is comprised by clean sands (1.31<Ic ≤ 2.05) and sands with low content of silts (2.05 < I_c ≤ 2.6). The deepest layer (found between 12 and 20m), is comprised by softer materials, with values of q_{c1Ncs} falling between 100 and 200.

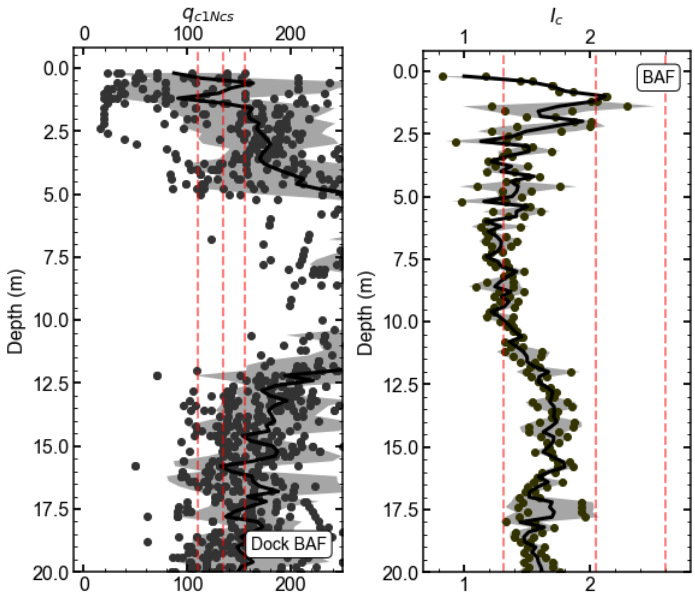

Figure 2. CPT profiles in terms of qc1Ncs and Ic for the site of wharf BAF, as interpreted from the tests executed by Facciorusso and Vannucchi (2003).

The baseline geotechnical model used for the 2D simulations is depicted in Figure 3. It was constructed after compiling the CPT data with the model developed Bozzoni et al. (2014).

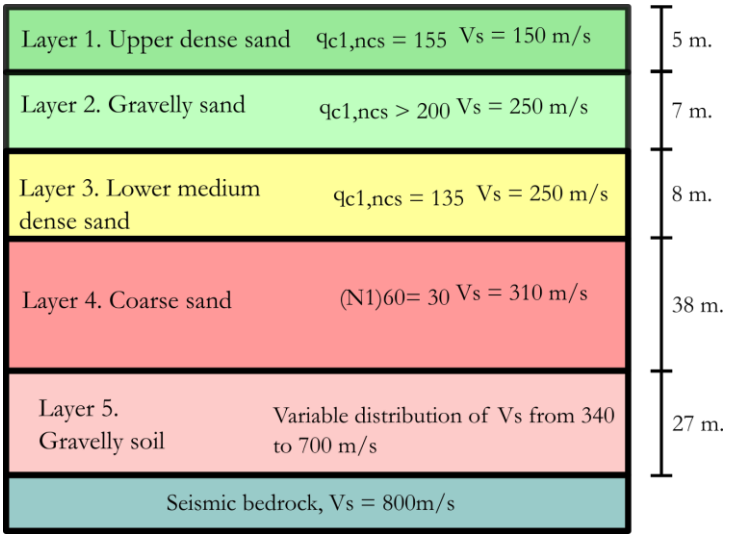

Figure 3. Baseline geotechnical profile used for the 2D numerical analyses.

Seismic hazard at the site

According to seismic hazard considered by the current building code of Italy, the port of Gioia Tauro is located on a zone with the highest seismicity. For a return period of 475 years, the median peak ground acceleration for outcropping rock and ground-levelled conditions (A_g) is 0.264 g. The area of the port, as well as most of Italy, is expected to be predominately affected by near source events (R < 30 km), and for the port,

magnitudes around 6.0 are expected. More precise information about the disaggregation of the seismic hazard at the port site is given in Table 1, as presented by Barani et al. (2009).

TR (yr)	Median peak ground acceleration Ag (g)	Mean magnitude $\bar{M}$	Mean source to site distance $\bar{R}$ (km)
975	0.355	5.77	10.6
475	0.264	5.97	8.41
200	0.146	6.15	7.15

Table 1. Seismic hazard for the municipality of Gioia Tauro.

Modelling approach

Dynamic-soil-structure interaction (DSSI) problems involve a wide range of phenomena, each with varying degrees of complexity. Therefore, selecting an appropriate modelling approach should be based on the significance of the quantities involved, the underlying physical phenomena, available field and laboratory data, and the numerical tools at hand. In this study, we used the "direct approach", which involves modelling both the superstructure and soil in the same numerical model. To accomplish this, we employed FLAC 2D, a commercial code from Itasca Consulting Group, Inc. This explicit finite difference solver is specifically designed for hydro-mechanical coupled problems in geotechnical engineering. Advanced constitutive models for liquefiable layers and the superstructure, coupled with numerical consideration of large deformations, were used to account for higher-order effects. Additionally, to analyze both kinematic and inertial DSSI effects, two models were considered: the full model including the wharf structure (referred to as the SS model), and a "free-field" model without the wharf (referred to as the FF model).

The 2D finite difference model of the target wharf structure is shown in Figure 4. The model is 254m wide so that it ensures the attainment of free field conditions far inland from the wharf. Likewise, the height of the model was chosen such that (due the stiffness contrasts of the materials involved) it minimizes the effect of spurious wave reflections at the base. The nonlinear behavior of the liquefiable layers was accounted for by the means of PM4SAND (Boulanger and Ziotopoulou, 2017), a critical-state-compatible bounding-surface-plasticity model. The wharf was in turn modelled using the distributed plasticity model proposed by Andreotti and Lai (2017). The model is tailored for DSSI problems to simulate the cyclic degradation of structural elements, and thus compatible with performance-based earthquake engineering principles.

The soil columns, displayed alongside the main grid in Figure 4, are utilized to enforce free field boundary conditions, in line with the Lysmer and Kuhlemeyer (1969) formulation. An outcropping rock motion is applied to the bottom of the 1D columns as input excitation. The base of the columns comprises the well-established viscous (or quiet) boundaries. However, as shown by Kausel (1988) and observed in this study, the viscous boundary alone does not meet static equilibrium, and is therefore inefficient for low-frequency motion, such as that arising from the sliding of the slope. To overcome this limitation, we applied the motion recorded at the bottom of the 1D columns to the base of the main grid. In other words, the input excitation represents a real-time deconvolved motion.

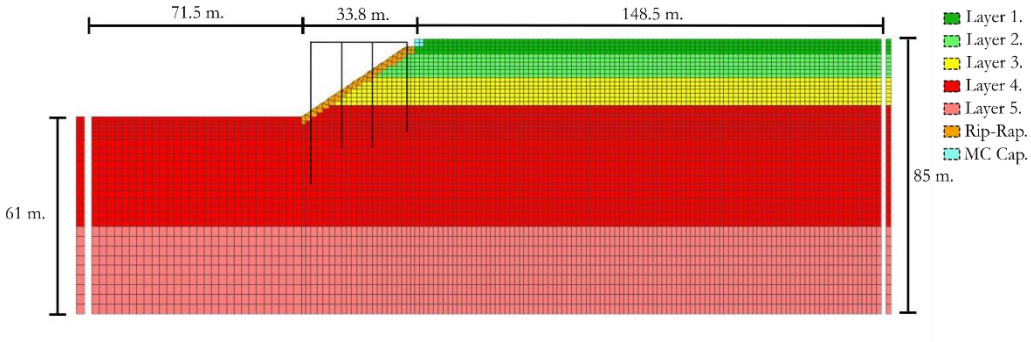

Figure 4. Finite difference model of the wharf structure of the port of Gioia Tauro

In terms of material modelling, the parameters of PM4SAND were calibrated based on q_{c1Ncs} values computed in the previous section. This was achieved by following the procedures laid down by Boulanger and Ziotopoulou (2017) and Ntritsos and Cubrinovsk (2020). Table 2 reports the selected parameters, while Figure 5 shows the verification of the model response against the liquefaction triggering criterion of Boulanger and Idriss (2014).

	Layer 1. Upper dense sand	**Layer 3. Lower medium to dense sand**
γ_d	1.68 g/cm^3	1.61 g/cm^3
D_r	0.75	0.6
G_o	650	950
h_{po}	0.2	
h_o	0.6	
ϕ_{cv}	32°	
e_{max}	0.79	
e_{min}	0.48	

Table 2. PM4SAND parameters used for the liquefiable layers.

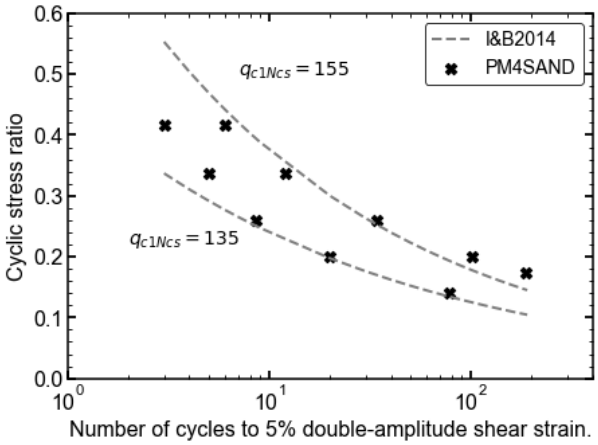

Figure 5.CPT-based calibration of PM4SAND.

A conventional elastic-perfectly-plastic Mohr-Coulomb model was used to model the non-liquefiable layers, except for Layer 5, which was assumed to be elastic. Table 3 provides details of the relevant material parameters utilized. To capture the non-linear characteristics more accurately, the analyses also incorporated the shear modulus and damping ratio curves proposed by Zhang et al. (2005) for the non-liquefiable layers.

	Riprap	Layer 2. Gravelly sand	Layer 4. Coarse sand
γ	2.19 g/cm^3	1.9 g/cm^3	1.9 g/cm^3
ϕ'	40	41	37
c'	20 kPa	5 kPa	5 kPa

Table 3. Mohr – Coulomb parameters used for the non-liquefiable soil layers.

In terms of structural modelling, plastic hinge zones were placed along the length of each pile to enforce the model of Andreotti and Lai (2017). The present study considered conventional reinforce concrete properties and detailing. The subsequent research stages will deal with more refined analyses in which the variability of the structural response is accounted for. As for the wharf deck, it was considered elastic and the mass of the crane is lumped to it. Shafieezadeh (2011) showed that the latter assumption has limited effects on the estimated response of the wharf, however it is inappropriate if the crane-wharf interaction is of interest.

The earthquake ground motion used in our analysis was chosen based on its compatibility with a TR (return period) of 475. Figure 6 displays the accelerogram of the mainshock from the 2016 Mw=6.5 central Italy earthquake, which was recorded at station MZ50. The station is situated on hard soil, and thus the motion was classified as outcropping-rock, with a PGA of 0.2. To conduct three analyses at different intensity levels, the motion was rescaled to correspond with the PGAs reported in Table 1.

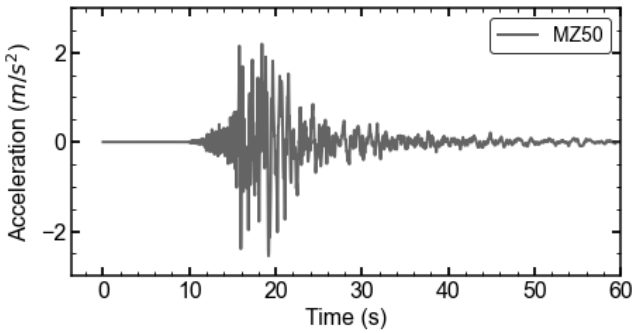

Figure 6. Acceleration time history of 2016 M_w=6.5 central Italy event recorded at the station MZ50.

Seismic response and global mode of failure.

Contours of the final displacement obtained from numerical analyses on both FF and SS models, using the T_R = 950 yr input motion, are presented in Figure 7. In the absence of the wharf, high shear strains concentrate at the slope's toe, and failure propagates through the gravel layer until it meets the bottom liquefiable layer. Beyond this point, the deformation pattern resembles that of a lateral spreading ground failure. In fact, the excess pore-water-pressure ratios shown in Figure 7 indicate that liquefaction of the bottom medium dense sand is triggered for the two highest intensity levels (PGA_{input} equal to 0.26g and 0.35g), but not for the lowest (PGA_{input} equal to 0.14g).

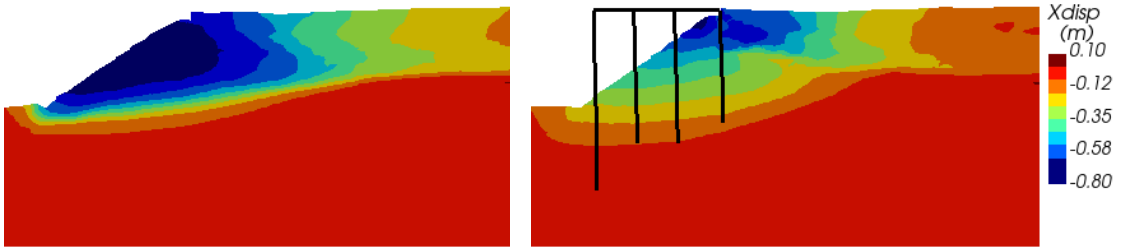

Figure 7. Contours of final horizontal displacements for the model without (FF) and with (SS) the inclusion of the piles; left and right panes respectively.

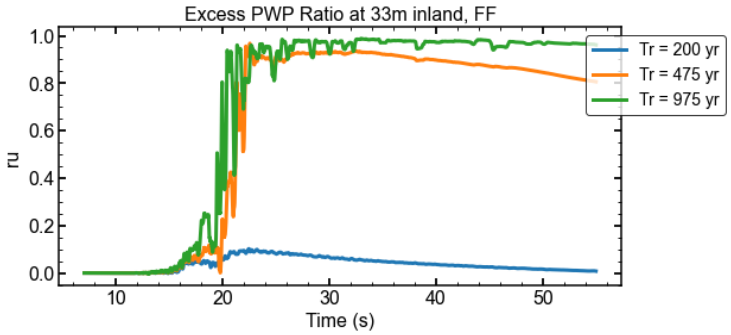

Figure 8. Excess Pore Water Pressure ratios computed at the midpoint of the medium dense sand layer 33m inland from the wharf, for the FF model.

The inclusion of the wharf had three distinct effects on the overall response of the structure. Firstly, the piles helped to stabilize the slope by limiting excessive deformations from occurring at the toe. Secondly, the piles acted to restrain the laterally spreading ground, reducing the magnitude of lateral displacements inland from the wharf. However, in contrast, the upper portion of the slope experienced large displacements, with magnitudes as large as those in the FF case, due to the significant ground strains induced by the motion of the wharf. Figure 9 provides a more detailed analysis of the opposing effects arising from the inclusion of the piles. It compares the final horizontal displacements recorded at the toe and crest of the slope. As can be seen, the pile-pinning effects at the toe occur at all three earthquake intensity levels considered. However, at the crest, this beneficial effect is not observed. For instance, for a PGA_{input} value of 0.26 (corresponding to a T_R of 475 years), the crest displacement was greater with the presence of the wharf than without it.

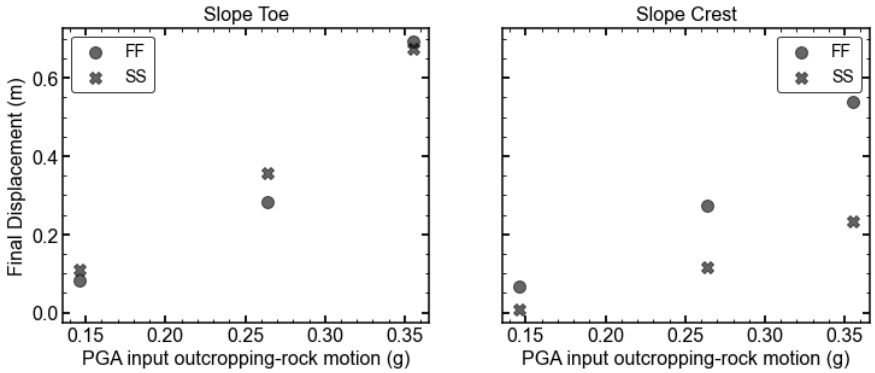

Figure 9. Comparison of final horizontal displacements reported at the toe and crest of the submerged slope computed from the FF and SS analyses, and for three different intensity levels of the input excitation.

Seismic performance and estimated demands for the trailing pile.

The lateral capacity of the wharf is primarily dependent on the trailing pile due to, on one hand, its shorter free length, and on the other, its relatively longer embedment. Therefore, the discussion will focus on the seismic response and demands of the trailing pile alone. To this end, ten plastic zones were distributed along the pile length using the formulation of Andreotti and Lai (2017). Figure 10 illustrates the moment-rotation diagrams for the pile-deck and in-ground (at 10m depth) plastic zones at two intensity levels: T_R=475 yr and TR=950 yr. The in-ground hinge response is similar to that of a monotonic loading case, with minimal loading reversals. On the other hand, the pile-deck hinge undergoes more loading cycles and experiences greater deformations. It's worth noting that at these intensity levels, liquefaction of the bottom layer is triggered. Therefore, the seismic demand on the pile at 10m depth is mainly influenced by kinematic effects.

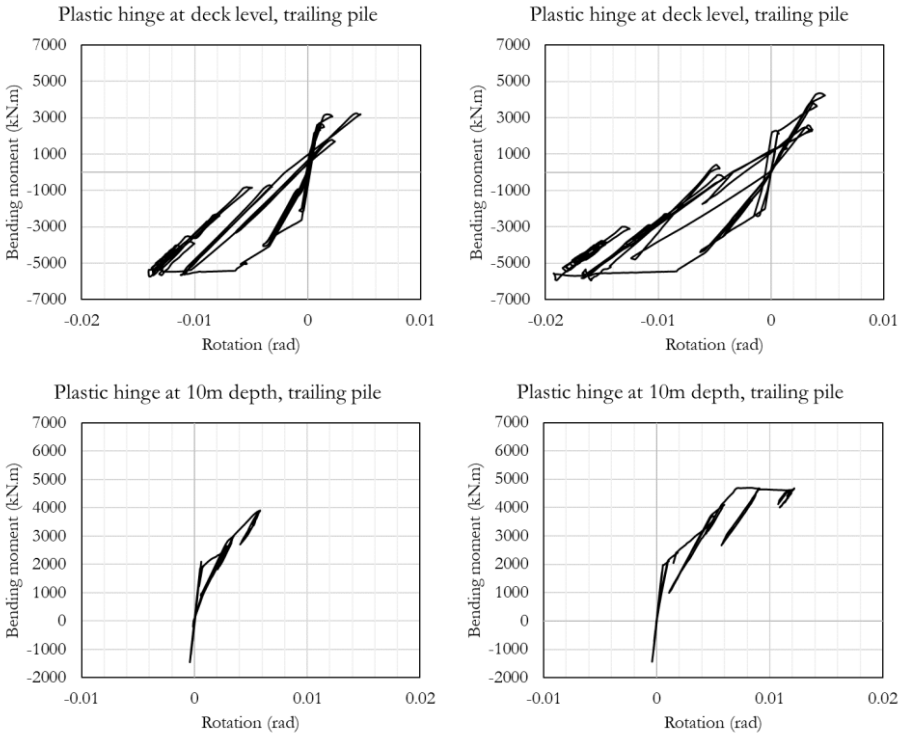

Figure 10. Response of the pile-deck and in-ground (10m depth) plastic zones of the trailing pile for two differing intensity levels; T_R = 475 yr, right panels, T_R = 950 yr, left panels.

Figure 11 shows the distributions of bending moment, final horizontal displacement, and ductility demand for the trailing pile. The latter is defined as the ratio between the maximum rotation reported by the 2D analysis and the yield rotation obtained from sectional analysis. Bending moment and final horizontal displacement profiles for T_R = 475 yr were omitted for the sake of readability. They showed a similar trend to that of T_R = 950 yr, they exhibited a similar trend to TR = 950 yr with smaller peak values.

As observed previously, at higher seismic intensities, the medium-to-dense sand experiences liquefaction in both the FF and SS analyses. In the FF analysis, the displacement distributions along the pile axis are primarily influenced by the lateral movement of the liquefiable layer. This leads to the formation of a plastic zone within the dense sand, as depicted in the left panel of Figure 11. Conversely, for the lower intensity motion (TR = 200 yr), the bending moment distribution indicates a minimal presence of kinematic effects. In this scenario, the demand on the pile is primarily driven by the inertial forces transmitted by the deck, resulting in yielding at the pile-deck hinge only.

Finally, Table 4 contains a summary of the estimated demands. In general, as the intensity of the input excitation is increased, the inertial effects play a less significant role. The peak acceleration attained at the deck level goes from 0.24 to 0.29g for the lower intensity and remains unchanged for the highest. In contrast, the deck displacement and the ductility demand on the ground hinge increased dramatically, from 36 cm to 63 cm for the former, and from 1.44 to 3.04 for the former.

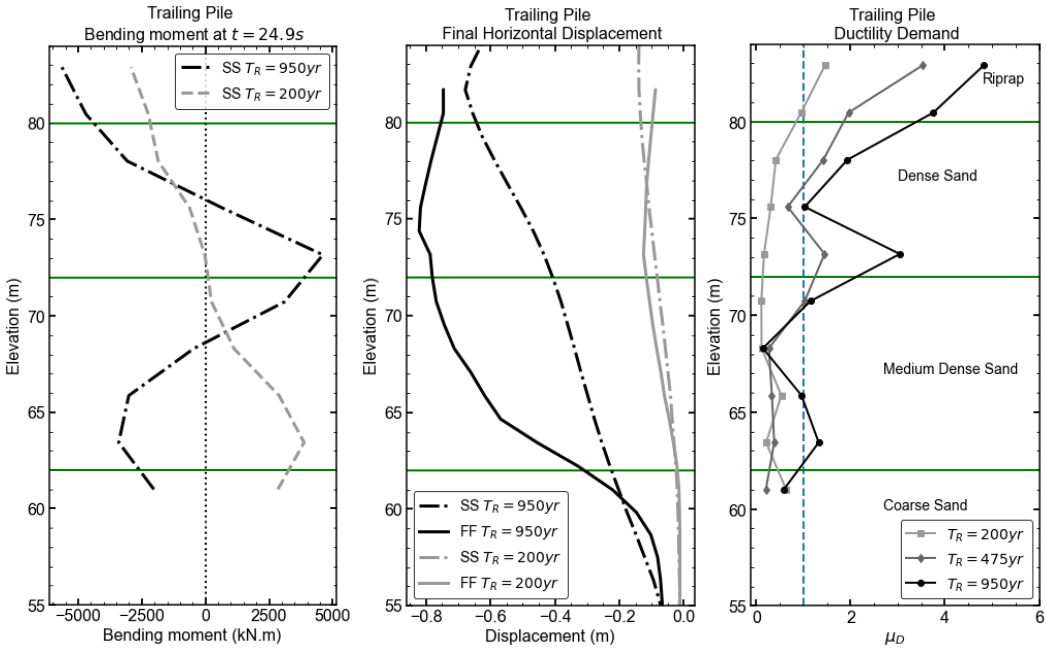

Figure 11. Distributions of bending moment, ground displacements and ductility demand for the trailing pile.

Tr (yr)	Δ_{deck} (m)	PGA_{deck} (g)	M_{max} Pile-deck PH (kN.m)	M_{max} 10 m depth PH (kN.m)	μ_d Pile-deck PH	μ_d 10 m depth PH
200	0.016	0.24	4851	1813	1.46	0.16
475	0.36	0.29	5726	3901	3.56	1.44
950	0.63	0.29	5943	4700	4.8	3.04

Table 4. Summary of the seismic demands estimated for the trailing pile

Concluding remarks

This study aimed to investigate the seismic response of a large-diameter pile-supported wharf using dynamic time history analysis, which directly modelled the nonlinear response of both the soil and superstructure. The analyses allowed for the consideration of higher order effects that cannot be otherwise captured when the ground and the structure are modelled separately. We showed that the global response of the wharf was affected by complex dynamic soil structured interaction effects. Grouped into two kinematic and inertial effects, the first were found to be favorable to the overall stability of the wharf, while the latter were found to be detrimental.

In terms of the local response of the trailing pile, we observed that the kinematic and inertial interaction effects varied significantly with the intensity of the input motion. The mode of deformation of the wharf was determined by the earthquake intensity. When liquefaction and lateral spreading were triggered, the demand on the piles was mostly governed by kinematic effects. This suggests that, for design purposes, the combination of kinematic and inertial demand is determined by the target failure mode, which is in turn influenced by the local site conditions and ground motion intensity. Our results also showed that while inertial effects were dominant or as relevant as kinematic effects for lower ground motion intensities, they were overshadowed by the impact of lateral spreading on the pile.

Future work is necessary to address the uncertainty related to the various inputs and assumptions considered in this study, particularly regarding the epistemic uncertainty surrounding the response of liquefiable soils and the variability of soil properties. Additionally, further efforts are required to assess the suitability of simplified analysis approaches for reproducing the trends identified in this study.

Acknowledgements

The first author would like to express gratitude to the Eucentre Foundation for providing funding for this work in the form of a Ph.D. scholarship. Additionally, the authors would like to extend their appreciation to Professor Miko Cubrinovski and Dr. Riwaj Dhakal for their valuable insights and support provided throughout the various stages of this study.

References

Andreotti G and Lai CG (2017) A nonlinear constitutive model for beam elements with cyclic degradation and damage assessment for advanced dynamic analyses of geotechnical problems. Part I: theoretical formulation. *Bulletin of Earthquake Engineering* 15(7): 2785–2801. DOI: 10.1007/s10518-017-0090-1.

Barani S, Spallarossa D and Bazzurro P (2009) Disaggregation of Probabilistic Ground-Motion Hazard in Italy. *Bulletin of the Seismological Society of America* 99(5): 2638–2661. DOI: 10.1785/0120080348.

Boulanger RW and Idriss IM (2014) CPT and SPT Based Liquefaction Triggering Procedures. Report No. UCD/CGM-14/01. Center for Geotechnical Modeling, Department of Civil and Environmental Engineering, University of California, Davis.

Boulanger RW and Ziotopoulou K (2017) "PM4Sand (version 3.1): A sand plasticity model for earthquake engineering applications." Report No. UCD/CGM-17/01. Center for Geotechnical Modeling, Department of Civil and Environmental Engineering, University of California, Davis, CA.

Bozzoni F, Famà A, Lai CG, et al. (2014) Seismic Risk Assessment Of Seaports Using Gis: The Port Of Gioia Tauro In Southern Italy. *PIANC World Congress San Francisco, USA 2014*.

Conca D, Bozzoni F and Lai CG (2020) Interdependencies in Seismic Risk Assessment of Seaport Systems: Case Study at Largest Commercial Port in Italy. *ASCE-ASME Journal of Risk and Uncertainty in Engineering Systems, Part A: Civil Engineering* 6(2): 04020006. DOI: 10.1061/AJRUA6.0001043.

Faccioli E and Vanini M (2003) Complex seismic site effects in sediment-filled valleys and implications on design spectra. *Progress in Structural Engineering and Materials* 5(4): 223–238. DOI: 10.1002/pse.156.

Facciorusso J and Vannucchi G (2003) LIQUEFACTION HAZARD MAPS OF THE HARBOUR AREA OF GIOIA TAURO (ITALY) BY GEO-STATISTICAL METHODS. *Proceedings of the 4th International Conference of Earthquake Engineering and Seismology, Tehran, Islamic Republic of Iran*: 9.

Famà A, Bozzoni F and Lai CG (2014) Valutazione in ambiente GIS del danno sismico distrutture portuali marittime: il caso del porto di Gioia Tauro. *Progettazione Sismica* (2): 49–72. DOI: 10.7414/PS.5.2.49-72.

Itasca Consulting Group, Inc (2019) FLAC- Fast Lagrangian Analysis of Continua, Ver. 8.1.

Kausel E (1988) Local Transmitting Boundaries. *Journal of Engineering Mechanics* 114(6): 1011–1027. DOI: 10.1061/(ASCE)0733-9399(1988)114:6(1011).

Lysmer J and Kuhlemeyer RL (1969) Finite Dynamic Model for Infinite Media. *Journal of Engineering Mechanics Division* 95(4).

Ntritsos N and Cubrinovski M (2020) A CPT-based effective stress analysis procedure for liquefaction assessment. *Soil Dynamics and Earthquake Engineering* 131: 106063. DOI: 10.1016/j.soildyn.2020.106063.

Robertson PK and Cabal, K. L. (2015) Guide to Cone Penetration Testing for Geotechnical Engineering. *Corporate Headquarters, Signal Hill, California*.

Shafieezadeh A (2011) Seismic Vulnerability Assessment of Wharf Structures. PhD Dissertation Giorgia Institute of Technology.

Zhang J, Andrus RD and Juang CH (2005) Normalized Shear Modulus and Material Damping Ratio Relationships. *Journal of Geotechnical and Geoenvironmental Engineering* 131(4): 453–464. DOI: 10.1061/(ASCE)1090-0241(2005)131:4(453).